

Influence of the Parameters of Disk Winding on the Impulse Voltage Distribution in Power Transformers

M. Heidarzadeh* and M. R. Besmi*(C.A.)

Abstract: Overvoltage distribution along the transformer winding must be uniform to certify the safety of the operation of the power transformer. Influence of the parameters variation on the Impulse Voltage Distribution (IVD) in disk winding transformer is going to be analyzed which hasn't been analyzed on this type of winding in the previous papers. In this research, a transformer with disk winding and rectangular cross-section is analyzed. Equations for capacitances between winding turns and also equations for capacitances between turns and core are deduced. Noting that the relationships presented are dependent on the parameters of the transformer winding, so with changing these parameters, the capacitances of turn –turn and turn – core and finally the capacitances of total series and parallel of the winding will be changed. The purpose of this paper is to show the effect of the variations of these parameters on the IVD in disk winding of transformer. This paper, will assess how to change the parameters of disk winding in order to achieve a uniform initial IVD along the winding and to reduce the Amplitude of Impulse Voltage Fluctuations (AIVF) in winding and which parameters have more effect in making uniform the IVD on the disk winding.

Keywords: Constant of Winding Voltage Distribution, Disk Winding, Impulse Voltage Distribution, Series and Parallel Capacitances.

1 Introduction

Frequency pattern of impulse voltage caused by lightning contains fundamental frequencies up to several megahertz. Thus, in these high frequencies, capacitances of transformer winding should be considered in calculations. But they ignored in power frequency [1-3]. These capacitances are considered between windings and grounded components (i.e. core, tank, etc) and between disks, layers and turns. With presence of these capacitances, IVD along the winding isn't uniform. Non-uniform IVD along the winding produces severe stress on the winding which can be resulted in electric breakdown of transformer insulation. In power frequency, voltage distribution along the winding is uniform and there is not stress on the transformer insulation. Therefore, IVD on the winding disks must be uniform in order to reduce the AIVF.

Distribution of the impulse voltage along the winding depends on the winding capacitive network that is consisting of parallel and series capacitances [1]. Capacitors between winding turns are known as series

and capacitors between turns and core are known as parallel capacitors.

According to Fig. 1, the voltage of any point in capacitive network in the time of the strike of impulse voltage, U , with assuming the transformer winding is grounded is deduced from Eq. (1) [3]:

$$V(x) = U \left(\frac{e^{\alpha x} - e^{-\alpha x}}{e^{\alpha l} - e^{-\alpha l}} \right) \quad (1)$$

where

$$\alpha = \sqrt{\frac{C_p}{C_s}} \quad (2)$$

In Eq. (1), U is the amplitude of the applied impulse voltage to the winding terminal, l is the total length of winding and x is the coordinates of point for calculating the voltage. Also in Eq. (2), C_s is the total series capacitance of the winding, and C_p is the total parallel capacitance of the winding.

Constant of winding voltage distribution (α) shows the rate of uniformity of IVD along the transformer winding [1]. This coefficient depends on the total series and parallel capacitance of winding. Total series capacitance of the winding is equivalent to the capacitances of turn-turn and total parallel capacitance of the winding is equivalent to the capacitances of turn-core.

Iranian Journal of Electrical & Electronic Engineering, 2014.

Paper first received 7 July 2013 and in revised form 6 Oct. 2013.

* The Authors are with the Electrical and Electronic Engineering Department, Shahed University, Tehran, Iran.

E-mails: mhzadeh14@yahoo.com and besmi@shahed.ac.ir.

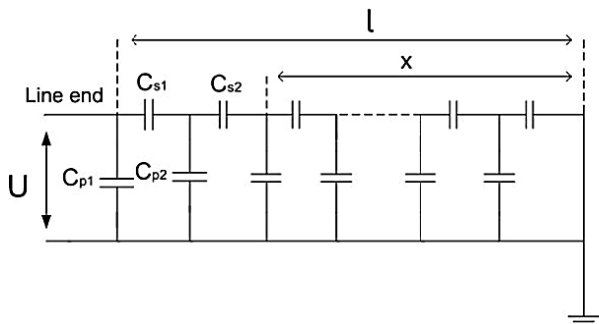


Fig. 1 Capacitive network of the transformer winding in time of the strike of the impulse voltage U .

According to Eq. (2), by increasing α , the proportion of total series capacitance to the total parallel capacitance will decrease and according to the Fig. 2, causes the curve of IVD on the transformer winding to be nonlinear and also according to Fig. 3, AIVF on the winding will be increased.

By decreasing the coefficient α , not only IVD on the winding uniforms but also AIVF in the winding reduces.

According to Fig. 2, the winding of a transformer has been analyzed for several cases. If in capacitive network of the winding, the proportion of total series to parallel capacitance be small ($\alpha=10$), the curve of IVD will be non-linear. But if the proportion of total series to parallel capacitance in capacitive network be big ($\alpha=1$), the curve of IVD will be linear. Also, in $\alpha=0$, the curve of the IVD will change to a straight line.

Fig. 2 shows, the initial IVD on a grounded winding for different α [1]. Also Fig. 3 shows the maximum voltage gradient on each disk of the winding at the time of transient fluctuations (curve of AIVF) with respect to different values of α [1].

According to the above sentences, to minimize the damage to the winding in the time of the strike of impulse voltage, the coefficient of α must be the smallest possible value. Methods of interleaving the winding turns and use of the electrostatic shielding in windings, are used for linearization of the initial IVD on the winding and for reducing α [4-7].

In [8], voltage distribution and maximum electric field intensity in power transformer windings, using various electric shields are studied. In [9], the methods of computing the equivalent series capacitance of a unit coil for transient analysis in large transformers are presented.

In [10], describes the application of the concept of fractal geometry to obtain the features inherent in the impulse response of transformers subjected to impulse test. In [11], studies effect of new suggested ferro-resonance limiter on controlling ferro-resonance oscillation in the power transformer including Metal Oxide Surge Arrester (MOSA). Also [12], presents feasible methods for mitigation of the overvoltage

magnitude. In [13], presents a simple analytic formula for calculating the disk capacitance with a variable number of wound-in-shield turns. In [14]-[19], presents methods of calculating the series and parallel capacitances (turn-turn and turn-core capacitances) of capacitive network of the winding. The phenomenon of magnetizing inrush in a transient condition was studied in [20].

The purpose of this paper is to associate the capacitive model of the winding to the capacitive equations related to the winding dimensions, insulation and core. Unlike the other papers, the voltage distribution on the winding is studied; but in this paper the effects of different winding dimensions, insulations and core which were not mentioned in the previously studies have been presented in this paper. It is noteworthy that the dimensions of winding, insulations and core are the parameters of capacitive equations.

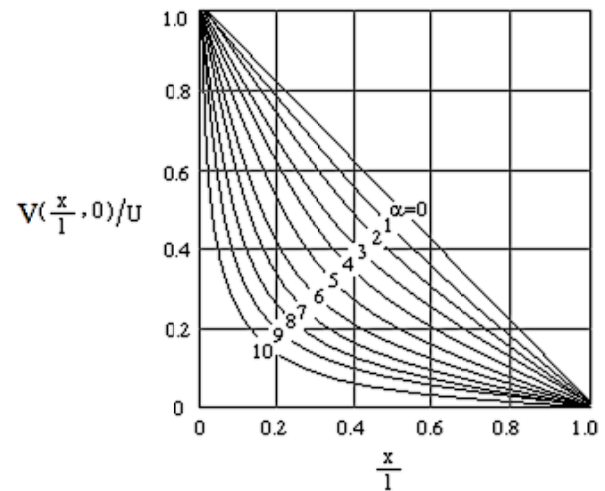


Fig. 2 Impact of α on the initial impulse voltage distribution.

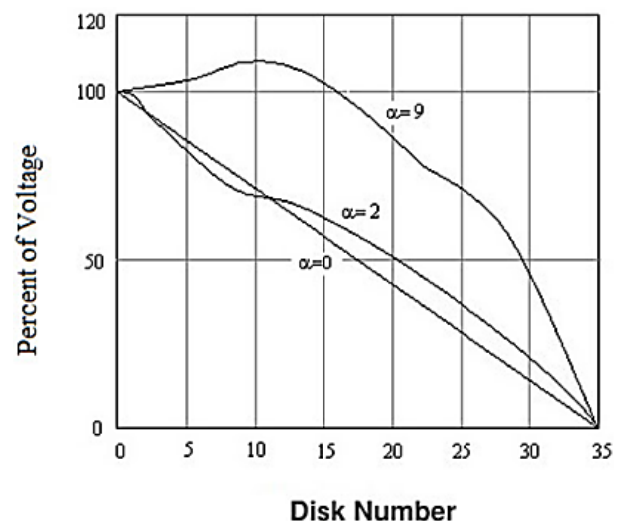


Fig. 3 Impact of α on the amplitude of the impulse voltage fluctuations.

Series and parallel capacitances in capacitive network of the winding depend on parameters of the winding. So these parameters can be useful in making the distribution of initial impulse voltage more uniform and also have effect on reduction of the AIVF on the winding.

In this paper, the influence of winding parameters on the IVD has been studied. With the results of this paper, we can understand how to change the winding parameters in order to achieve a uniform initial IVD and reduce the AIVF along the transformer winding and also to understand which parameters will have a more effect to make uniform the IVD on winding. Also in this research, changes in each parameter of the winding for decreasing the impulse voltage on each disk have been analyzed. In this paper, capacitive network of disk winding is being studied. We also assume that winding has rectangular cross-section. The winding of a typical transformer has been studied using VOLNA software [4-7] and [21]. Program of Calculation of Impulse Voltages in Transformer Winding (VOLNA) is professional software which is used in the company of Iran Transformer [21].

2 Calculating Series and Parallel Capacitance

2.1 Series Capacitance

In this section equations for series capacitors (turn-turn capacitors) will be presented. In Fig. 4 a coil with rectangular winding is shown. For calculating the capacitance we neglect the curvature of the turns and assume the conductors are straight with unlimited length. Two conductors with rectangular cross-section which are straight and parallel are equivalent to two parallel planes. From the parallel-plane capacitor equation we have:

$$C = K \cdot \epsilon_0 \frac{A}{d} \quad (3)$$

In Eq. (3), A is the cross-section of parallel planes, d is distance of between two parallel planes, ϵ_0 is the permittivity of vacuum and K is a constant for winding leakage effects.

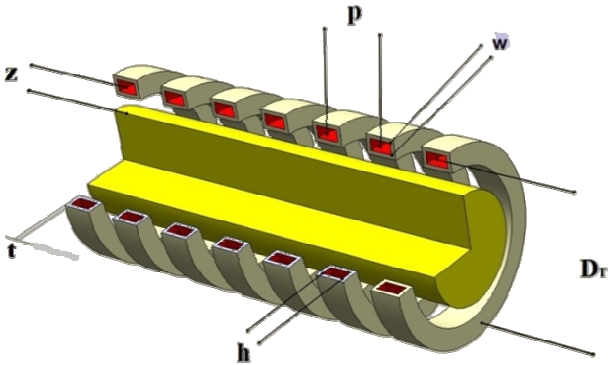


Fig. 4 View of a coil with rectangular cross-section of turns.

In next steps Eq. (3) will be more accurate so that winding parameters will be included. In this method [14-19], distance between two adjacent turns or the turn and core are divided into different parts. According to Fig. 5, distance between two adjacent turns is divided into 3 regions. First region is the insulating coating of the first turn, second region is the insulation between adjacent turns and the third region is the insulating coating of the second turn.

The capacitance for the insulating coating of each wire (capacitance of the first and third regions) is calculated from Eq. (4) that is deduced using Eq. (3).

$$C_{ic} = \epsilon_0 \cdot \epsilon_r \cdot \frac{\pi \cdot D_T \cdot w}{t} \quad (4)$$

Parameters of Eq. (4) are shown in Fig. 4. In this equation, D_T is the average diameter of the turn, w is the width of turn's cross-section without insulating coating and t is the thickness of the insulating coating on one side and ϵ_r is the relative permittivity of the insulating coating of each wire.

In transformer windings, the insulation between the two turns is usually oil. The capacitance between two adjacent turns in the area of covered by oil (capacitance in the second region) from Eq. (5) is calculated:

$$C_{oil} = \epsilon_0 \cdot \epsilon_{r(oil)} \cdot \frac{\pi \cdot D_T \cdot w}{p - h - 2t} \quad (5)$$

In Eq. (5), p is winding pitch or distance between centers of the cross-sections of the adjacent turns, h is the height of turn's cross-section without insulating coating and $\epsilon_{r(oil)}$ is the relative permittivity of oil.

The distance between two adjacent turns in the transformer winding, in addition to the oil can include other insulations, which is ignored from them. In the distance of between two adjacent turns, the capacitance associated with the first region and the capacitance associated with the second region and the capacitance associated with the third region, make up a series composition that the orientation of this series combination is shown in Fig. 6.

This series combination can be shown as Eq. (6):

$$C_{tt} = \frac{C_{ic} \cdot C_{oil}}{C_{ic} + 2C_{oil}} \quad (6)$$

It is important to note that the capacity of associated with the first and third regions are equal. By substituting Eqs. (4) and (5) in Eq. (6), the total capacitance between two adjacent turns (turn-turn capacitor) using Eq. (7) is calculated:

$$C_{tt} = \epsilon_0 \cdot \epsilon_{r(oil)} \cdot \frac{\pi \cdot D_T \cdot w}{p - h - 2t \left(1 - \frac{\epsilon_{r(oil)}}{\epsilon_r} \right)} \quad (7)$$

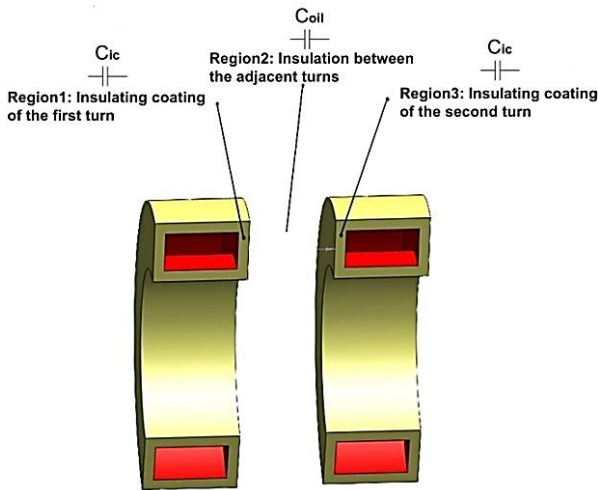


Fig. 5 Regions between two adjacent turns.

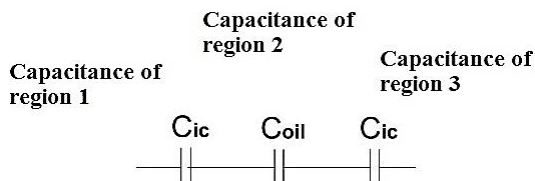


Fig. 6 Series combination of capacitances in the distance of between two adjacent turns.

2.2 Parallel Capacitance

For calculation of parallel capacitance (turn-core capacitor), like section 2.1 the curvature of the turns are ignored. Also the core is considered as a plane. Also the core is considered as a plane. Also in this section the basic equation is Eq. (3) which will be more accurate later. In this method [14-19], the distance between the turn and the core is divided into two regions. According to Fig. 7, first region is the insulating coating of the turn and the second region is the insulation between turn and core (oil).

In this section, for calculation of the capacitance of first region (the capacitance of insulating coating of the turn) is used from Eq. (8):

$$C_{ic} = \epsilon_0 \cdot \epsilon_r \cdot \frac{\pi \cdot D_T \cdot h}{t} \quad (8)$$

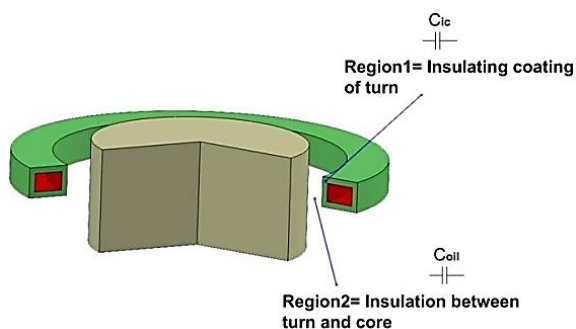


Fig. 7 Regions between turn and core.

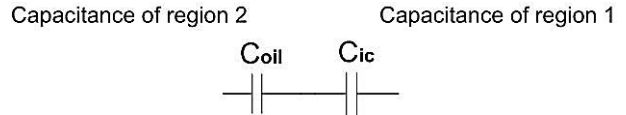


Fig. 8 Series combination of capacitances in the distance of between turn and core.

Capacitance of second region (i.e. the region filled with oil) is calculated according to the Eq. (9):

$$C_{oil} = \epsilon_0 \cdot \epsilon_{r(oil)} \cdot \frac{\pi \cdot D_T \cdot h}{Z - (w/2) - t} \quad (9)$$

Parameters of Eq. (9) are shown in Fig. 4. In this equation, Z is distance between the center of turn's cross-section and the outer surface of the core. According to Fig. 8, in the distance between the turn and core capacitance associated with the first region make a series combination with the capacitance associated with the second region.

This series combination can be shown as Eq. (10):

$$C_{ic} = \frac{C_{ic} \cdot C_{oil}}{C_{ic} + C_{oil}} \quad (10)$$

It should be noted that in this section, there is only one capacitor C_{ic} but in section of 2.1 there were two capacitors C_{ic} which were series. So by substituting Eqs. (8) and (9) in Eq. (10), the total capacitance between the turn and core (turn-core capacitor) using Eq. (11) is calculated:

$$C_{ic} = \epsilon_0 \cdot \epsilon_{r(oil)} \cdot \frac{\pi \cdot D_T \cdot h}{Z - (w/2) - t \left(1 - \frac{\epsilon_{r(oil)}}{\epsilon_r} \right)} \quad (11)$$

Eqs. (4) - (11) are based on references [14-19].

3 Study of Capacitive Network of the Disk Winding

In Fig. 9, view of a disk winding is shown. In this type of winding, each disk has several turns that are placed in one horizontal plane. In this winding, the turns

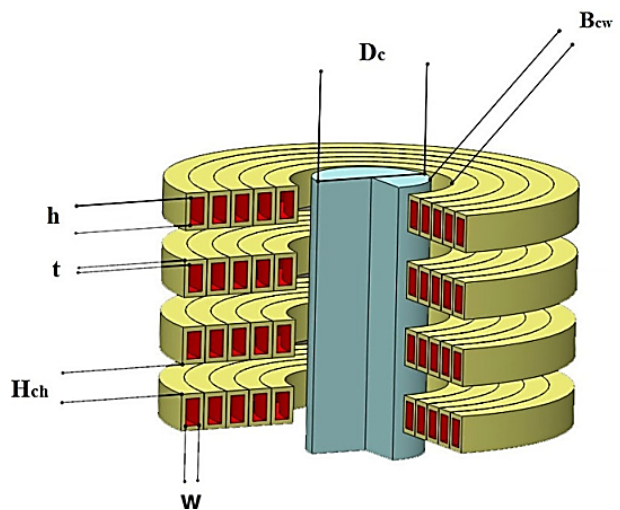


Fig. 9 Disk winding with 4 disks that each disk has 5 turns.

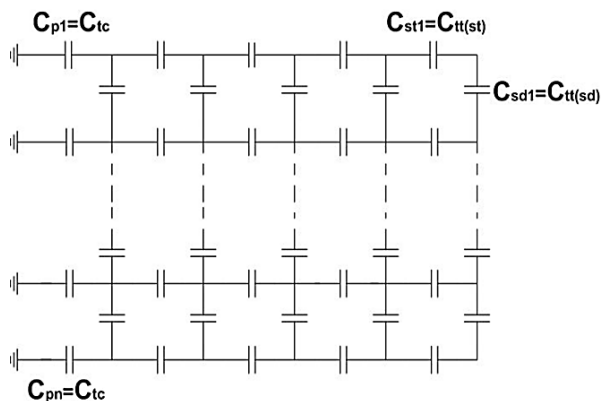


Fig. 10 Capacitive network of the disk winding.

of first disk are wrapped from outside to inside and next disk is wrapped in different direction (from inside to outside) and this procedure is repeated to final disk.

The advantages of disk winding is that they can be used in high power and high voltage transformers and provide high cooling capability, mechanical strength and good impulse voltage distribution.

Capacitive network of the disk winding is shown in Fig. 10. In this capacitive network, there are two kinds of series capacitors and one kind of parallel capacitor. Series capacitors are as follow:

- 1- Turn-Turn capacitors, between adjacent turns in one disk ($C_{tt(st)}$).
- 2- Turn-Turn capacitors, between adjacent turns in two adjacent disks ($C_{tt(sd)}$).

Also Turn-Core capacitors (C_{tc}) in disk winding are as a parallel capacitor.

Series capacitors in the capacitive network of the disk winding from Eq. (7) and parallel capacitors from Eq. (11) are calculated. Proportional to change in each parameter of the winding, one or more parameters in Eqs. (7) and (11) will be changed and caused to change the capacitive network of the winding. With variations in the capacitive network of the winding, the IVD and AIVF on the winding and also the impulse voltage on each disk will be changed.

4 Impulse Voltage Distribution Analysis on the Disk Winding

A typical transformer with disk winding is considered for this section. The parameters of the transformer winding are introduced in Table 1.

The results of the change in winding parameters according to VOLNA software are shown in the following tables and figures. Figures 11-14 which are based on Fig. 2 show how the IVD on the winding changes as the parameters of winding change. Tables 2-5 show the change of impulse voltage on each disk of the winding as the winding parameters variation (voltage on each disk is a percent of applied impulse voltage).

By increasing the distance of the core outer surface from the winding (B_{cw} , D_T in Eqs. (7) and (11) and also Z in Eq. (11) will be increased. This variation causes to increase the proportion of total series to total parallel capacitances. According to Fig. 11, these variations will be caused the IVD on the winding to be uniform and it will be also decreased α . Also from Table 2 it can be seen that with increasing B_{cw} , the impulse voltage on each disk was decreased. Thus the risk of electrical breakdown is reduced in the winding insulation.

Table 1 Parameters of simulated disk winding.

Number of disks (N)	20
Number of turns in each disk (n)	4
Relative permittivity of insulation	Paper=4.2 oil=2.25
Height of turn's cross-section without insulating coating (h)	9.5 mm
Width of turn's cross-section without insulating coating (w)	6.5 mm
Thickness of paper insulation of the conductor in one side(t)	0.5 mm
Diameter of core (D_c)	500 mm
Distance of the outer surface of the core to winding (B_{cw})	30 mm
Length of the channel between winding's disks (H_{ch})	4.5 mm

Table 2 Changes of the impulse voltage on the disks caused by the changes of B_{cw} .

Disk Number	Impulse voltage on the disks [%]			
	$B_{cw}=10$ mm	$B_{cw}=30$ mm	$B_{cw}=50$ mm	$B_{cw}=80$ mm
1	100.21	97.79	97.02	96.82
2	100.29	97.19	96.33	96.06
3	100.85	93.31	91.43	90.76
4	100.90	92.75	90.70	89.99
5	100.00	88.67	84.78	83.99
6	99.87	88.07	83.88	83.08
7	96.85	83.11	77.53	75.80
8	96.27	82.36	76.69	74.70
9	90.77	76.04	69.99	66.02
10	89.85	75.07	69.00	64.72
11	81.54	67.41	61.17	56.96
12	80.23	66.26	59.99	55.87
13	68.99	56.71	51.36	46.89
14	67.31	55.24	50.09	45.57
15	53.32	44.11	39.40	34.97
16	51.28	42.47	37.75	33.40
17	34.44	28.93	24.90	21.73
18	32.15	26.86	23.01	20.04
19	13.76	11.13	9.42	8.17
20	11.01	8.85	7.48	6.48

Table 3 Changes of the impulse voltage on the disks caused by the changes of H_{ch} .

Disk Number	Impulse voltage on the disks [%]			
	$H_{ch}=0$ mm	$H_{ch}=4.5$ mm	$H_{ch}=10$ mm	$H_{ch}=20$ mm
1	99.99	97.79	99.99	99.99
2	91.85	97.19	99.08	100.57
3	91.85	93.31	99.08	100.57
4	83.56	92.75	97.943	100.32
5	83.56	88.67	97.94	100.32
6	74.93	88.07	94.67	97.76
7	74.93	83.11	94.67	97.76
8	65.94	82.36	89.17	91.91
9	65.94	76.04	89.17	91.91
10	56.41	75.07	80.59	83.37
11	56.41	67.41	80.59	83.37
12	46.84	66.26	69.39	71.57
13	46.84	56.71	69.39	71.57
14	35.74	55.24	55.42	56.77
15	35.74	44.11	55.42	56.77
16	23.66	42.47	39.16	39.59
17	23.66	28.93	39.16	39.59
18	11.71	26.86	20.57	20.96
19	11.71	11.13	20.57	20.96
20	2E-07	8.85	2E-07	2E-07

Table 4 Changes of the impulse voltage on the disks caused by the changes of t .

Disk Number	Impulse voltage on the disks [%]			
	$t=0.125$ mm	$t=0.5$ mm	$t=1.0$ mm	$t=1.5$ mm
1	97.53	97.79	98.07	98.33
2	96.77	97.19	97.56	97.90
3	91.63	93.31	94.41	95.25
4	90.90	92.75	93.95	94.87
5	85.56	88.67	90.30	91.53
6	84.78	88.07	89.76	91.01
7	78.90	83.11	85.21	86.68
8	78.04	82.36	84.50	86.02
9	71.32	76.04	78.27	79.93
10	70.33	75.07	77.31	78.99
11	62.46	67.41	69.60	71.00
12	61.29	66.26	68.40	69.82
13	52.47	56.71	58.56	59.79
14	51.16	55.24	57.07	58.27
15	40.09	44.11	45.48	46.16
16	38.40	42.47	43.86	44.49
17	25.47	28.93	30.04	30.69
18	23.57	26.86	27.91	28.56
19	9.72	11.13	11.58	11.90
20	7.73	8.85	9.21	9.46

As it is seen from Fig. 12, with decreasing the length of the channel between winding's disks (H_{ch}), the IVD along the winding will be more uniform, that means the

AIVF on the winding will be decreased. This is because by reducing the H_{ch} , P in Eq. (7) will be reduced and the total series capacitance will be increased. The decrease of impulse voltage on each disk with decreasing H_{ch} in the Table 3 can be observed.

Decreasing the thickness of paper insulation of the conductor (t) has a little effect on the IVD of the disk winding. Since in the capacitive network of disk winding the number of series capacitances is more than the parallel capacitances, the decrease of t has more effect on the value of total series capacitance. So with the decrease of t , the proportion of total series to total parallel capacitances will increase and according to Fig. 13, the IVD along the winding become linear but it is not significant. Also according to Table 4, the impulse voltage on disks will decrease by decreasing t .

To analyze IVD on the winding with respect to changing the dimensions of conductor cross-section, it has been tried to consider the area of conductor cross-section to be constant but with changing its height (h) and width (w). According to Fig. 14, the most uniform IVD on the disk winding can be seen that when the cross-section of each turn of disk has its maximum h and its lowest w . Also Table 5 shows the impulse voltage variation on each disk of winding for various values of w and h .

Table 5 Changes of the impulse voltage on the disks caused by the changes of w and h .

Disk Number	Impulse voltage on the disks [%]			
	$w=2, h=30.875$ mm	$w=30.875, h=2$ mm	$w=6.5, h=9.5$ mm	$w=9.5, h=6.5$ mm
1	97.98	98.15	97.79	96.97
2	97.32	97.54	97.19	96.19
3	92.66	93.25	93.31	90.95
4	91.97	92.62	92.75	90.22
5	86.35	87.93	88.67	85.06
6	85.49	87.26	88.07	84.31
7	78.76	82.12	83.11	78.54
8	77.77	81.35	82.36	77.68
9	70.37	75.26	76.04	70.92
10	69.28	74.35	75.07	69.92
11	60.85	66.99	67.41	62.16
12	59.59	65.88	66.26	61.00
13	49.77	56.96	56.71	51.92
14	48.32	55.60	55.24	50.55
15	37.65	44.74	44.11	40.05
16	36.15	43.10	42.47	38.51
17	24.13	29.70	28.93	26.01
18	22.34	27.72	26.86	24.11
19	9.17	11.90	11.134	9.93
20	7.287	9.62	8.85	7.90

In Fig. 15, the maximum and minimum of impulse voltage on the second disk of the winding for various parameters (in Table 1), has been shown. These values have been taken from Tables 2-5 for the second disk.

As it is observed from Fig. 15, the decrease of H_{ch} has the most impact on decreasing of impulse voltage on the second disk.

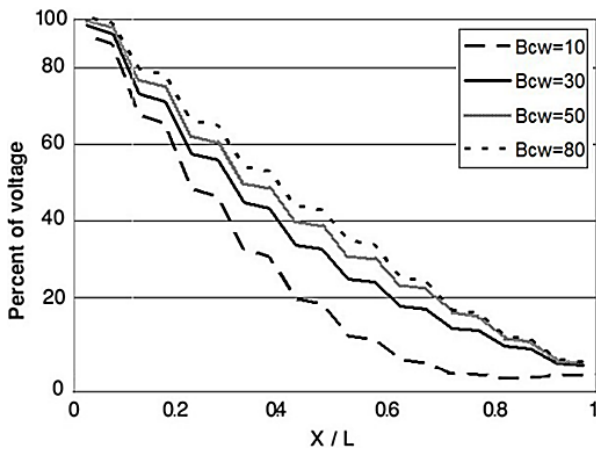


Fig. 11 Changes of IVD on the winding caused by the changes of B_{cw} .

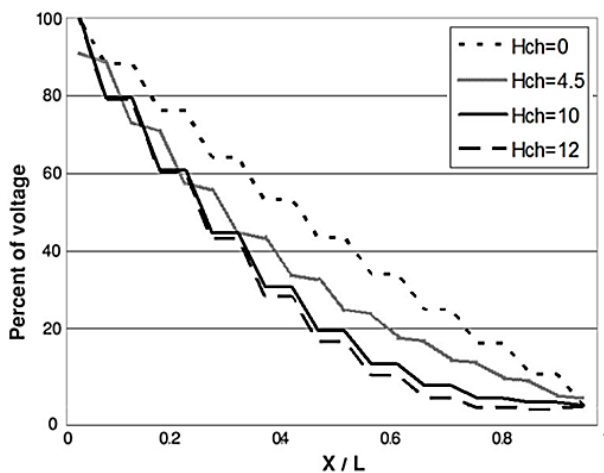


Fig. 12 Changes of IVD on the winding caused by the changes of H_{ch} .

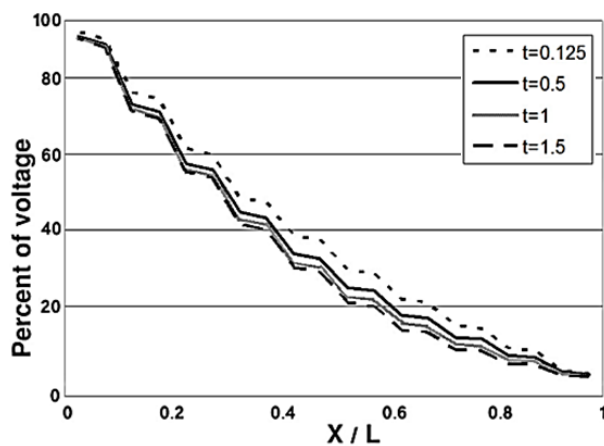


Fig. 13 Changes of IVD on the winding caused by the changes of t .

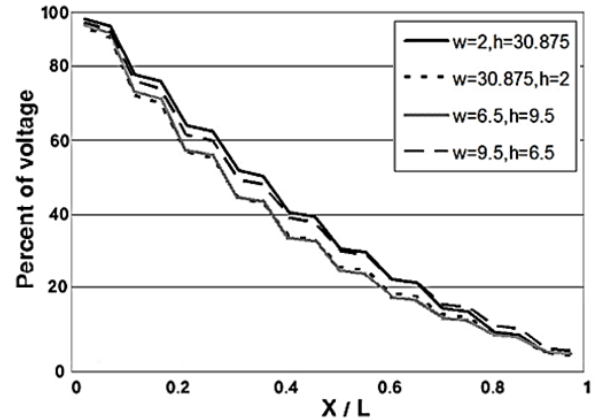


Fig. 14 Changes of IVD on the winding caused by the changes of w and h .

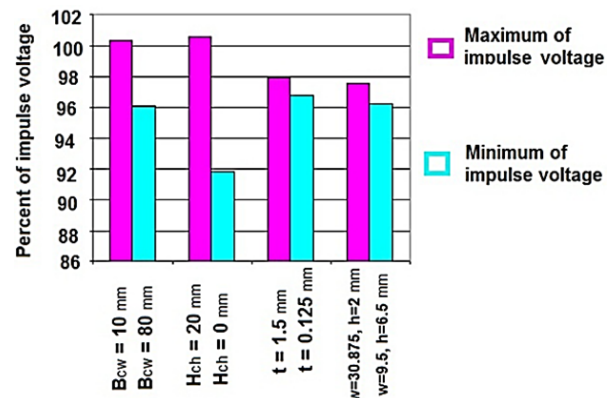


Fig. 15 Max and min of the impulse voltage on the second disk for the various parameters.

5 Conclusions

In this paper, a typical transformer with disk winding and with the introduced parameters was modeled using software VOLNA and then with changing the parameters of the winding by this software, the variations of the impulse voltage distribution on the winding and the rate of the variation of impulse voltage on each disk of the winding were analyzed. In this study, a disk winding with rectangular cross-section was considered.

In the curves obtained from the software, reducing the amplitude of impulse voltage fluctuations means to reduce the constant of winding voltage distribution and reduction in these two factors means a more uniform impulse voltage distribution along the winding.

In this paper was shown that a change in each parameter of the winding causes the capacitive network and the proportion of total series to parallel capacitance to change and this will cause a change in impulse voltage distribution of the winding.

It was observed that the thickness of paper insulation of the conductor has lowest effect on impulse voltage distribution of the winding but the increase of the distance of the core outer surface to the winding and the

decrease of the length of the channel between disks will improve impulse voltage distribution along the winding.

This result was also obtained that if in the cross-section of each turn of disk the height (on metal) be maximum and the width (on metal) be minimum, the most uniform of the impulse voltage distribution on the disk winding will be obtained.

References

- [1] K. Karsai and D. Kerényi, *Large Power Transformer*, New York: Elsevier, 1987.
- [2] A. Greenwood, *Electrical Transients in Power Systems*, 2nd ed., New York: Wiley, 1991.
- [3] S. V. Kulkarni and S. A. Khaparde, *Transformer Engineering Design and Practice*, New York: Marcel Dekker, INC., 2004.
- [4] M. Bagheri, A. Hekmati, R. Heidarzadeh and M. Naderi, "Impulse voltage distribution in intershield disk winding VS interleaved and continuous disk winding in power transformer", *IEEE International Conf. on Power and Energy*, pp. 387-392, December 2008.
- [5] M. Bagheri, M. Vakilian, A. Hekmati and R. Heidarzadeh, "Influence of electrostatic shielding of disc winding on increasing the series capacitance in transformer", *IEEE Lausne Powertech*, pp. 1780-1784, 2007.
- [6] M. Bagheri, M. Vakilian and A. Hekmati, "Simulation and comparison of primary surge voltage distribution in simple disk winding, disk winding with complete shield and interleaved winding in power transformers", *22th Power System Conf. (PSC)*, 2007.
- [7] M. Bagheri, M. Vakilian and A. Hekmati, "Using electrostatic shields rather than interleaving windings in order to increase windings series capacitors in power transformers", *21th Power System Conf. (PSC)*, 2006.
- [8] M. R. Meshkatodini, A. Shahmohammadi, M. Majidi and M. Karami, "Comparative study of the effect of various shields on lightning electric field in power transformer windings", *IEEE Trondheim Power Tech.*, June 2011.
- [9] L. Yan, D. Jianping, L. Xiaohui and L. Dongxue, "Calculation of capacitance and inductance parameters based on FEM in high-voltage transformer winding", *IEEE Int. Conf. on Electrical Machines and Systems (ICEMS)*, 2011.
- [10] C. Koley, P. Purkait, S. Chakravorti, D. Brahma, M. Ghanti, B. Pratihari and S. Saha, "Fractal-ANN tool for classification of impulse faults in transformers", *IEEE Indicon*, pp. 152-156, 11-13 Dec. 2005.
- [11] H. Radmanesh and M. Rostami, "Impacts of new suggested ferroresonance limiter on the stability domain of ferroresonance modes in power transformers considering metal oxide surge arrester effect", *Iranian Journal of Electrical & Electronic Engineering*, Vol. 7, No. 4, pp. 283-291, Dec 2011.
- [12] A. Tavakoli and A. Gholami, "Mitigation of transient over voltages generated due to switching operations and lightning in gas-insulated substation (GIS) without extra limiter", *Iranian Journal of Electrical & Electronic Engineering*, Vol. 7, No. 3, pp. 190-196, Sep. 2011.
- [13] R. M. DelVecchio, B. Poulin and R. Ahuja, "Calculation and measurement of winding disk capacitances with wound-in-shields", *IEEE Trans. on Power Delivery*, Vol. 13, No. 2, pp. 503-509, April 1998.
- [14] L. Dalessandro, F. Silveira and J. W. Kolar, "Self-Capacitance of high-voltage transformers", *IEEE Trans. Power Electronics*, Vol. 22, No. 5, pp. 2081-2092, Sep. 2007.
- [15] G. Grandi, M. K. Kazimierczuk, A. Massarini and U. Reggiani, "Stray capacitances of single-layer solenoid air-core inductors for high-frequency applications", *IEEE Conf. Industry Applications*, pp. 1384-1388, Sep. 1996.
- [16] G. Grandi, M. K. Kazimierczuk, A. Massarini and U. Reggiani, "Stray capacitances of single-layer solenoid air core inductors", *IEEE Trans. Industry Applications*, Vol. 35, No. 5, pp. 1162-1168, Sep./Oct. 1999.
- [17] M. E. Mosleh and M. R. Besmi, "Sensitivity analysis and stray capacitance of helical flux compression generator with multilayer filamentary conductor in rectangular cross-section", *Iranian Journal of Electrical & Electronic Engineering*, Vol. 8, No. 1, pp. 55-67, March 2012.
- [18] M. E. Mosleh and M. R. Besmi, "Stray capacitance of a magneto cumulative generator including N-turn, single-layer, solid, and round conductor with insulating coating", *IEEE Trans. on Plasma Science*, Vol. 39, No. 10, pp. 1990-1997, Oct. 2011.
- [19] M. E. Mosleh and M. R. Besmi, "Calculation of stray capacitances of MCG coil include one turn, single-layer and conductor wire filaments in rectangular form", *Iranian Journal of Electrical & Electronic Engineering*, Vol. 7, No. 1, pp. 19-27, March 2011.
- [20] M. Jamali, M. Mirzaie and S. A. Gholamian, "Discrimination of inrush from fault currents in power transformers based on equivalent instantaneous inductance technique coupled with finite element method", *Iranian Journal of Electrical & Electronic Engineering*, Vol. 7, No. 3, pp. 197-202, Sep. 2011.
- [21] OSC "VIT" (Ukraine) Company, *Program of Calculation of Impulse Voltages in Transformer Winding (VOLNA)*, 1995-2001.



Mojtaba Heidarzadeh was born in Sari, Iran, in 1986. He received the B.Sc. degree in electrical engineering from Babol Noshirvani University of Technology, Iran, in 2009. Now, he studies M.Sc in electrical engineering at Shahed University, Iran. His research interests are high voltage engineering and transformer calculations. Now, he is

working at the Department of Transformer, Iran Transformer Research Institute, in section of transformer calculations.



Mohammad Reza Besmi was born in Tehran, Iran, in 1959. He received the B.Sc. degree in electrical engineering from Amirkabir University, Iran, in 1989, the M.Tech degree in electrical engineering from University of Indian Institute of Technology, Delhi in June 1992 and the Ph.D. degree in electrical engineering from Newcastle upon Tyne

University in September 1996. From 1997 to 1999, he was with the Niroo Research Institute in Iran. He is currently Assistant Professor of Electrical Engineering Department. His current research work is in special electrical machine design.